Analyses of a continuum traffic flow model for a non-lane-based system

Arvind Kumar Gupta* and Isha Dhiman
Department of Mathematics, Indian Institute of Technology Ropar,
Rupnagar-140001, Punjab, India.
*akgupta@iitrpr.ac.in

Abstract: We develop a heterogeneous continuum model based upon a car-following model for a non-lane-based system taking lateral separation into account. The criterion for linear stability analysis and traveling wave solution of the homogeneous case is studied. The consideration of the lateral separation not only stabilizes the flow but also shrinks the critical region. For heterogeneous case, the fundamental diagram is examined for two different equilibrium speed-density functions and the effect of lane width is investigated for different compositions of heterogeneous traffic. The theoretical findings agree well with the results of numerical simulation which justifies the applicability of the model to a non-lane-based system.

Keywords: Non-lane-based; Traffic flow; Stability; Heterogeneous; Continuum model

PACS Nos.: 45.70.Vn, 46.15.-x

1. Introduction

In the past few decades, the development of various traffic flow models has received considerable attention. The goal of studying traffic flow is to reduce traffic congestion and hence, to optimize the flow. The traffic behavior can be analyzed using theoretical as well as experimental approaches. The theoretical approach includes development of efficient models to understand the real-world complex traffic phenomena.

Continuum traffic models belong to an important class of macroscopic models which are derived from the analogy between vehicular flow and fluid flow. These models describe the collective behavior of traffic using macroscopic variables flow, density and velocity. The simplest continuum model in literature is the first-order model independently given by Lighthill and Whitham[1] and Richards[2]. Later, several modifications of Lighthill-Whitham-Richards (LWR) model are proposed in the literature of traffic flow theory. [3-9]

In recent years, researchers have mainly focused on two types of generalizations of existing traffic flow models. One kind of generalization is developing multi-lane models in which motion of vehicles in individual lanes is considered. Another way to generalize, which has gained much attention, is distinction between various classes of vehicles. It is expected that incorporating the concept of distinguished vehicle classes and their respective flow characteristics into traffic flow models yields more accurate and realistic results as compared to contemporary single-class models. In this aspect, Hoogendoorn and Bovy[10] presented a multi-class model using the principles of gas dynamics. Wong and Wong[11] extended LWR model by incorporating the multi-class concept. Ngoduy *et al.*[12] formulated a multi-lane and multi-class model considering traffic conditions in urban areas. Laval and Daganzo[13] developed a hybrid multi-lane model and discussed the lane changing effects. Gupta and Katiyar[14] proposed an anisotropic continuum model for multi-class vehicles. Logghe and Immers[15] presented multi-class kinematic wave model in which vehicle classes interact in a non-cooperative way.

Due to tremendous increase in automobiles, roads in developing countries are becoming strongly congested day by day. The traffic flow in these countries is heterogeneous and highly disordered. Here, the word heterogeneous traffic indicates the presence of more than one type of vehicle. A disordered traffic system is one where vehicles do not follow lane system and try to move ahead by utilizing the lateral space. As a result, vehicles in such systems have not one, but several leaders. Classical continuum models have limitations to fully understand the complexities arising due to real-world disordered traffic conditions. This stimulates the need of developing a model which efficiently describes the mixed traffic phenomena more realistically over a non-lane-based system.

In the literature, very limited studies have been recorded to develop an understanding of traffic flow for non-lane-based heterogeneous or mixed traffic conditions. Jin *et al.*[16] presented a non-lane-based full velocity difference (FVD) car-following model and described the effects of lane-width on traffic flow. Recently, Nair *et al.*[17] used porous flow approach to formulate a multi-class model for disordered heterogeneous traffic. In the proposed methodology[17], vehicles use the lateral space as pores which help to increase the traffic flow. The main drawback of Nair's approach is that the analytical relationship between areal density and vehicles' class composition with pore space is not known explicitly. Later, Peng *et al.*[18] proposed a non-lane-based lattice hydrodynamic model by incorporating the lateral separation effects of the lane width. Up to our knowledge, no efforts have been made in the past to develop higher-order continuum traffic flow models for a non-lane-based system, which is the motivation for the present work.

In section 2, we apply the relationship between micro and macro variables to develop a non-lane-based continuum heterogeneous model based on the car-following model given by Jin *et al.*[16] and discuss its mathematical properties. In section 3, we analyze the homogeneous model qualitatively for traveling wave solution. Section 4 discusses the numerical results and the effect of lateral separation distance parameter on various traffic conditions. We then analyze the equilibrium curve and the situation of traffic jam under the effect of lateral separation in section 5. Finally in section 6, we provide a discussion on our results.

2. Model Development

The car-following theory was developed to model the motion of vehicles following each other on a single lane without overtaking. It is believed that the vehicles travel in the middle lane and each vehicle is influenced by the one in its front. However, as pointed out by Gunay[19], in developing countries like India and China, not every vehicle is positioned on the centre of the lane, which results in lateral separations between the leaders and the followers. Jin *et al.*[16] incorporated the lateral separation characteristics on a single-lane highway and presented a non-lane-based full velocity difference homogeneous car-following model. In this model, the dynamic state of the following vehicle depends on the lateral separation effects of its leader. Though this model can describe some complex phenomena of real traffic but does not suit to study the heterogeneous traffic conditions as the effect of probability of each vehicle class on the car-following behavior is not considered.

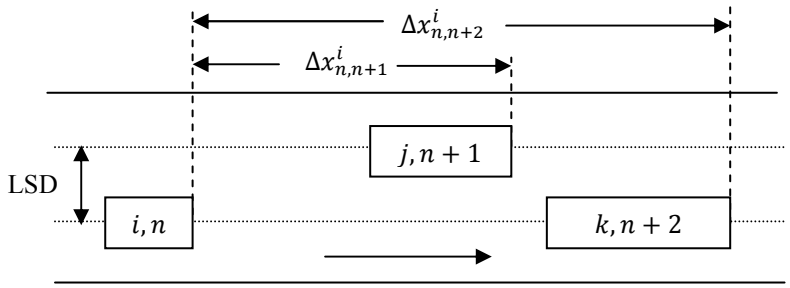

Fig. 1. A typical car following situation on a non-lane-based system

Fig. 1 shows a typical non-lane-based car following situation in which due to off-central positions of the vehicles, the following vehicle does not assign leadership fully to the vehicle in its front. Under this situation, the following vehicle has a possibility to overtake the leading vehicle although the overtaking does not occur. Here, (i,n), $(j,n+1)$ and $(k,n+2)$ denote that the n^{th}, $(n+1)^{th}$ and $(n+2)^{th}$ vehicles are respectively, the i-class, j-class and k-class. The probability that the leading vehicle of the vehicle (i,n) is the j-class is p_{ij}.

Taking into account the effect of probabilities of each class on heterogeneous traffic flow, we present a modified non-lane-based full velocity difference model in which the dynamic equation of the n^{th} vehicle is represented by the following equation:

$$\frac{dv_n^i(t)}{dt} = \alpha_i\{V_i[\Delta x_{n,n+1}^i(t), \Delta x_{n,n+2}^i(t)] - v_n^i(t)\} + \kappa_i G[\Delta v_{n,n+1}^i(t), \Delta v_{n,n+2}^i(t)] \quad i = 1,2,3 \ldots\ldots N \qquad (1)$$

where $$V_i[\Delta x_{n,n+1}^i(t), \Delta x_{n,n+2}^i(t)] = V_i[(1-\delta_n)\Delta x_{n,n+1}^i(t) + \delta_n \Delta x_{n,n+2}^i(t)]$$

and $$G[\Delta v_{n,n+1}^i(t), \Delta v_{n,n+2}^i(t)] = (1-\delta_n)\Delta v_{n,n+1}^i(t) + \delta_n \Delta v_{n,n+2}^i(t)$$

Here, $v_n^i(t)$ is the velocity of (i,n) vehicle at time t; $V_i(.)$ is the optimal velocity of the vehicle (i,n); N is the total number of classes; κ_i is the sensitivity coefficient of response to the stimulus $G(.)$; α_i is the sensitivity coefficient of i-class driver to the difference between its optimal and current velocities and $\Delta x_{n,n+1}^i(t)$ is the headway of vehicle (i,n), which can be computed as a mean of the random variables $x_{n+1}^j(t) - x_n^i(t)$ as

$$\Delta x_{n,n+1}^i(t) = \sum_{j=1}^N p_{ij}\left(x_{n+1}^j(t) - x_n^i(t)\right) \qquad (2)$$

Similarly, the relative velocity between vehicle $(j, n+1)$and vehicle (i,n) at time t is given by

$$\Delta v_{n,n+1}^i(t) = \sum_{j=1}^N p_{ij}\left(v_{n+1}^j(t) - v_n^i(t)\right) \qquad (3)$$

It is clear from Eq. (1) that the velocity, spacing and sensitivity coefficients of each class affect the dynamics of the vehicle (i,n). The lateral separation distance parameter for n^{th} vehicle i.e. δ_n can be computed as the ratio of lateral separation distance (LSD) between n^{th} and $(n+1)^{th}$ vehicle and the maximal lateral separation distance[16]. Larger the value of δ_n, more easily n^{th} vehicle will overtake $(n+1)^{th}$ vehicle and follow $(n+2)^{th}$ vehicle. When $\delta_n = 0$, it means that there is no lateral separation between n^{th} and $(n+1)^{th}$ vehicle and the model (1) will become the simplified FVD model for heterogeneous traffic. When $\delta_n = 1$, n^{th} and $(n+1)^{th}$ vehicles are on different lanes and in this case, n^{th} vehicle will actually follow $(n+2)^{th}$ vehicle.

2.1. *A non-lane-based heterogeneous continuum model*

To develop the continuum model corresponding to the non-lane-based car-following model given by Eq. (1), we assume that the n^{th} vehicle at position x represents the average traffic condition at $\left(x - \left(\Delta_j/2\right), x + \left(\Delta_j/2\right)\right)$. Here Δ_j is the distance between the leading and following vehicles. We adopt the method[18] to transform the discrete variables of individual vehicles into the continuous flow variables as follows:

$$V_i[\Delta x_{n,n+1}^i(t), \Delta x_{n,n+2}^i(t)] \to \bar{V}_i\left(\frac{\rho}{1+\delta_n}\right),\ \alpha_i \to \frac{1}{T_i},\ \kappa_i \to \frac{1}{\tau_i},\ v_n^i(t) \to v_i(x,t),$$
$$v_{n+1}^j(t) \to v_j(x+\Delta_j, t),\ p_{ij} \to p_j(x+\Delta_j, t),\ \delta_n \to \delta \qquad (4)$$

Here, $\bar{V}_i(.)$ is the equilibrium speed of the i-class vehicle and $\rho = \sum_{i=1}^N \rho_i$ is the total density, where $\rho_i(x,t)$and $v_i(x,t)$ are density and speed of i-class vehicle, respectively at the point (x,t); T_i and τ_i are

reactive coefficients; $p_j(x+\Delta_j,t)$is the proportion of the j-class at point $(x+\Delta_j,t)$. Since computation of $p_j(x+\Delta_j,t)$ is complex as it is totally related to structure of heterogeneous traffic flow, so for simplicity, we assume $p_j(x+\Delta_j,t)=p_j(x,t)$.

Applying Eq. (4) to Eq. (1), we obtain

$$\begin{aligned}\frac{dv_i}{dt}=\frac{1}{T_i}\left[\bar{V}_i\left(\frac{\rho}{1+\delta}\right)-v_i\right]\\ +\frac{1}{\tau_i}\Bigg[(1-\delta)\sum_{j=1}^{N}p_j(x,t)\left(v_j\left(x+\Delta_j,t\right)-v_i(x,t)\right)\\ +\delta\sum_{j=1}^{N}p_j(x,t)\left(v_j\left(x+2\Delta_j,t\right)-v_i(x,t)\right)\Bigg]\end{aligned} \tag{5}$$

Using Taylor series, we rewrite it as

$$\begin{aligned}\frac{dv_i}{dt}=\frac{1}{T_i}\left[\bar{V}_i\left(\frac{\rho}{1+\delta}\right)-v_i\right]\\ +\frac{1}{\tau_i}\Bigg[(1-\delta)\sum_{j=1}^{N}p_j(x,t)\left(v_j\left(x+\Delta_j,t\right)-v_i(x,t)+v_j(x,t)-v_j(x,t)\right)\\ +\delta\sum_{j=1}^{N}p_j(x,t)\left(v_j\left(x+2\Delta_j,t\right)-v_i(x,t)+v_j(x,t)-v_j(x,t)\right)\Bigg]\end{aligned} \tag{6}$$

Expanding the right-hand side of Eq. (6) and neglecting the higher-order terms, we get

$$\begin{aligned}\frac{dv_i}{dt}=\frac{1}{T_i}\left[\bar{V}_i\left(\frac{\rho}{1+\delta}\right)-v_i\right]\\ +\Bigg[(1-\delta)\sum_{j=1}^{N}p_j(x,t)\left(c_j\frac{\partial v_j}{\partial x}+\frac{1}{\tau_i}\left(v_j(x,t)-v_i(x,t)\right)\right)\\ +\delta\sum_{j=1}^{N}p_j(x,t)\left(2c_j\frac{\partial v_j}{\partial x}+\frac{1}{\tau_i}\left(v_j(x,t)-v_i(x,t)\right)\right)\Bigg]\end{aligned} \tag{7}$$

To complete the model, we collect the terms on the right-hand side of Eq. (7) and expand left-hand side as

$$\frac{\partial v_i}{\partial t}+v_i\frac{\partial v_i}{\partial x}=\frac{1}{T_i}\left[\bar{V}_i\left(\frac{\rho}{1+\delta}\right)-v_i\right]+(1+\delta)\sum_{j=1}^{N}c_jp_j(x,t)\frac{\partial v_j}{\partial x}+\frac{1}{\tau_i}\sum_{j=1}^{N}p_j(x,t)\left(v_j(x,t)-v_i(x,t)\right) \tag{8}$$

where $c_j={}^{\Delta_j}/_{\tau_i}$ measures the propagation speed of the j-class vehicles at which a small change in traffic density propagates due to i-class vehicles.

Combining the above equation with the conservation equation, we obtain a non-lane based continuum model for heterogeneous traffic flow as:

$$\frac{\partial U}{\partial t} + \frac{\partial [f(U)]}{\partial x} = S(U) \tag{9}$$

where $U = \begin{pmatrix} \rho_1 \\ v_1 \\ \rho_2 \\ v_2 \\ \dots \\ \rho_N \\ v_N \end{pmatrix}$, $f(U) = \begin{bmatrix} \rho_1 v_1 \\ \frac{{v_1}^2}{2} - \sum_{j=1}^{N}(1+\delta)p_j c_j v_j \\ \rho_2 v_2 \\ \frac{{v_2}^2}{2} - \sum_{j=1}^{N}(1+\delta)p_j c_j v_j \\ \vdots \\ \rho_N v_N \\ \frac{{v_N}^2}{2} - \sum_{j=1}^{N}(1+\delta)p_j c_j v_j \end{bmatrix}$

and $S(U) = \begin{pmatrix} 0 \\ \frac{1}{T_1}\left[\bar{V}_1\left(\frac{\rho}{1+\delta}\right) - v_1\right] + \frac{1}{\tau_1}\sum_{j=1}^{N} p_j(x,t)\left(v_j(x,t) - v_1(x,t)\right) \\ 0 \\ \frac{1}{T_2}\left[\bar{V}_2\left(\frac{\rho}{1+\delta}\right) - v_2\right] + \frac{1}{\tau_2}\sum_{j=1}^{N} p_j(x,t)\left(v_j(x,t) - v_2(x,t)\right) \\ \vdots \\ 0 \\ \frac{1}{T_N}\left[\bar{V}_N\left(\frac{\rho}{1+\delta}\right) - v_N\right] + \frac{1}{\tau_N}\sum_{j=1}^{N} p_j(x,t)\left(v_j(x,t) - v_N(x,t)\right) \end{pmatrix}$

Note that if the lateral separation distance parameter i.e. $\delta = 0$, then the model reduces to the dynamic model of Tang *et al.*[20] and after taking $N = 1$, i.e. the homogeneous case, it converts into the speed gradient model[9] (SG model). Though, the driver's heterogeneity is not considered in this paper, yet it can better describe non-lane-based heterogeneous traffic flow.

2.2. *Mathematical properties*

Note that Eq. (9) represents system of governing equations for a heterogeneous system comprising of vehicles of N classes. Here, the system is written in conservative form. In order to discuss some important properties of the model, we write Eq. (9) in the following quasi-linear form.

$$\frac{\partial U}{\partial t} + J(U)U_x = S(U) \tag{10}$$

where $J(U)$ denotes the Jacobian matrix and is given by:

$$J(U) = \begin{bmatrix} v_1 & \rho_1 & 0 & 0 & \dots & 0 & 0 \\ 0 & v_1 - (1+\delta)p_1 c_1 & 0 & -(1+\delta)p_2 c_2 & \dots & 0 & -(1+\delta)p_N c_N \\ 0 & 0 & v_2 & \rho_2 & \dots & 0 & 0 \\ 0 & -(1+\delta)p_1 c_1 & 0 & v_2 - (1+\delta)p_2 c_2 & \dots & 0 & -(1+\delta)p_N c_N \\ \vdots & \vdots & \vdots & \vdots & \dots & \vdots & \vdots \\ 0 & 0 & 0 & 0 & \dots & v_N & \rho_N \\ 0 & -(1+\delta)p_1 c_1 & 0 & -(1+\delta)p_2 c_2 & \dots & 0 & v_N - (1+\delta)p_N c_N \end{bmatrix}$$

The eigen values of Jacobian matrix $J(U)$ are useful for determining the characteristics of partial differential equations in system (10). Based upon the eigen values of $J(U)$, we analyze an important property i.e. hyperbolicity of the system as follows.

2.3. *Hyperbolicity*

Let $\lambda_1, \lambda_2, \lambda_3$……., λ_N denote the eigen values of $J(U)$. The system of equations (10) is said to be strictly hyperbolic if all the eigen values of $J(U)$ are real and distinct[21]. Due to complexity of the model equations, it is difficult to compute the eigen values for more than two classes of vehicles. For simplicity, we have calculated the eigen values for *N*=2, for which the jacobian matrix takes the following form.

$$J(U) = \begin{bmatrix} v_1 & \rho_1 & 0 & 0 \\ 0 & v_1 - (1+\delta)p_1c_1 & 0 & -(1+\delta)p_2c_2 \\ 0 & 0 & v_2 & \rho_2 \\ 0 & -(1+\delta)p_1c_1 & 0 & v_2 - (1+\delta)p_2c_2 \end{bmatrix} \tag{11}$$

It is easy to obtain that

$$\lambda_1 = v_1\ , \lambda_2 = v_2$$
$$\lambda_3 = \frac{1}{2}\left(v_1 + v_2 - (1+\delta)p_2c_2 + \sqrt{\left((1+\delta)p_2c_2 + v_1 - v_2\right)^2 + 4p_1c_1v_2(1+\delta)}\right)$$
$$\lambda_4 = \frac{1}{2}\left(v_1 + v_2 - (1+\delta)p_2c_2 - \sqrt{\left((1+\delta)p_2c_2 + v_1 - v_2\right)^2 + 4p_1c_1v_2(1+\delta)}\right)$$

Note that, λ_i ; *i=1,2,3,4* are real and distinct. Therefore, governing model equations form a strictly hyperbolic system for which the eigen values indicate the characteristic speeds of propagation of solution. Unlike parabolic and elliptic system of equations, the hyperbolic system of partial differential equations propagates singularities. The hyperbolic nature of the system will be important in choosing a suitable numerical scheme for finding its solution.

3. Qualitative Properties of the Homogeneous Model

This section is devoted to analyze some qualitative properties of the proposed model for the homogeneous traffic case. The model equations governing the traffic flow on a unidirectional non-lane-based highway with homogeneous drivers are:

$$\frac{\partial \rho}{\partial t} + \frac{\partial(\rho v)}{\partial x} = 0 \tag{12}$$
$$\frac{\partial v}{\partial t} + v\frac{\partial v}{\partial x} = \frac{1}{T}\left[\overline{V}\left(\frac{\rho}{1+\delta}\right) - v\right] + (1+\delta)\lambda c\frac{\partial v}{\partial x} \tag{13}$$

where λ is a generic constant.

Note that if $\delta = 0$ and $\lambda = 1$, the model reduces to the SG model[8]. Although, the system (12) and (13) has a similar structure to SG models but is more general than these models. However, the differences are not the structural differences, so one would expect that our model behaves roughly the same as SG models and perhaps gives a more accurate description of traffic flow owing to its greater generality.

3.1. *Linear stability analysis*

The linear stability analysis is an important tool to investigate the system's behavior to small disturbances. We give a sufficiently small and smooth perturbation $(\hat{\rho}(x,t), \hat{v}(x,t))$ to a steady-state

solution $(\rho_0, \bar{V}(\rho_0))$ and examine the effect of lateral separation distance (LSD) parameter on the propagation of small disturbance. Substituting the small disturbances into the model equations (12) and (13) and collecting the linear terms after using the Taylor's series expansion at $(\rho_0, \bar{V}(\rho_0))$, we get

$$\frac{\partial \hat{\rho}}{\partial t} + \rho_0 \frac{\partial \hat{v}}{\partial x} + v_0 \frac{\partial \hat{\rho}}{\partial x} = 0 \tag{14}$$

$$\frac{\partial \hat{v}}{\partial t} + v_0 \frac{\partial \hat{v}}{\partial x} = \frac{1}{T}\left[\frac{\hat{\rho}}{1+\delta}\bar{V}'\left(\frac{\rho_0}{1+\delta}\right) - \hat{v}\right] + (1+\delta)\lambda c \frac{\partial \hat{v}}{\partial x} \tag{15}$$

To determine the stability condition for the system (14) and (15), we assume a specific type of disturbance given by

$$f(x,t) = \begin{pmatrix} \hat{\rho}(x,t) \\ \hat{v}(x,t) \end{pmatrix} = \begin{pmatrix} \hat{\rho}_0 \\ \hat{v}_0 \end{pmatrix} \exp\left[i(kx - \omega(k)t)\right] \tag{16}$$

Incorporating Eq. (16) into the system (14) and (15) and rewriting in the form

$$\begin{bmatrix} i(kv_0 - \omega) & ik\rho_0 \\ \frac{-\bar{V}'}{(1+\delta)T} & -i\omega + ikv_0 + \frac{1}{T} - ik(1+\delta)\lambda c \end{bmatrix} \begin{bmatrix} \hat{\rho}_0 \\ \hat{v}_0 \end{bmatrix} \exp[i(kx - \omega(k)t)] = 0 \tag{17}$$

For existence of non-trivial solutions of above system,

$$\begin{vmatrix} i(kv_0 - \omega) & ik\rho_0 \\ \frac{-\bar{V}'}{(1+\delta)T} & -i\omega + ikv_0 + \frac{1}{T} - ik(1+\delta)\lambda c \end{vmatrix} = 0 \tag{18}$$

Solving Eq. (18), we get

$$\omega^2 - \left(2kv_0 - (1+\delta)\lambda ck - \frac{1}{T}i\right)\omega - k^2 v_0 (1+\delta)\lambda c + k^2 {v_0}^2 - \frac{kv_0}{T}i - \frac{k\rho_0}{T}\frac{\bar{V}'}{(1+\delta)}i = 0 \tag{19}$$

Roots of Eq. (19) are given by

$$\omega = kv_0 - \frac{(1+\delta)\lambda ck}{2} - \frac{i}{2T}\left[1 \pm \sqrt{A + iB}\right] \tag{20}$$

where $A = 1 - (1+\delta)^2\lambda^2 c^2 k^2 T^2$ and $B = -2(1+\delta)\lambda ckT - \frac{4k\rho_0 \bar{V}'T}{(1+\delta)}$

As long as the imaginary part of ω is negative, the traffic flow will remain stable.

Define, $$\Omega(k) = Re\left[\sqrt{A + iB}\right] \tag{21}$$

For stability, $$|\Omega(k)| = (A^2 + B^2)^{\frac{1}{4}}\left(\frac{1+cos\varphi}{2}\right) < 1 \tag{22}$$

where $$\varphi = \arg\left(1 - (1+\delta)^2\lambda^2 c^2 k^2 T^2 - i\left(2(1+\delta)\lambda ckT + \frac{4k\rho_0 \bar{V}'T}{(1+\delta)}\right)\right) \tag{23}$$

For $|\Omega(k)|<1$, using (22), we get the stability criterion

$$\frac{\rho_0 \bar{V}'}{(1+\delta)^2} + \lambda c < 0 \tag{24}$$

It is to be noted that when $\delta = 0$ and $\lambda = 1$, the above stability criterion becomes similar to the one obtained for speed-gradient model using wavefront expansion technique by Ou[22]. Due to the presence of δ, the intermediate range of instability in the proposed model is different from SG model[9] which plays a crucial role in explaining the appearance of a 'phantom traffic jam' in real traffic.

3.2. *Travelling wave and shock*

The kinematic description of traffic flow includes the study of propagation of traffic disturbances in the form of traffic waves. A travelling wave is a stable, monotone and smooth wave form $(\rho, v)(x - St)$ travelling at a constant speed S and connecting two constant states $(\rho, v)(\pm\infty)$. We proceed by examining whether a traveling wave smooth solution for the proposed homogeneous model exists or not.

In order to determine the condition under which the given two constant states $(\rho, v)(\pm\infty)$ can be connected by a smooth travelling wave, we suppose that the proposed model admits a smooth travelling wave solution$(\rho, v)(x - St)$:

$$\rho = \rho(X) \text{ and } v = v(X) \text{ where } X = x - St \tag{25}$$

Substituting Eq. (25) into model (12) and (13), we get

$$-S\frac{\partial \rho}{\partial x} + \rho\frac{\partial v}{\partial x} + v\frac{\partial \rho}{\partial x} = 0 \tag{26}$$

$$-S\frac{\partial v}{\partial x} + \frac{\partial v}{\partial x} = \frac{1}{T}\left(\bar{V}\left(\frac{\rho}{(1+\delta)}\right) - v\right) + (1+\delta)\lambda c\frac{\partial v}{\partial x} \tag{27}$$

On integrating Eq. (26), we get

$$v = S + \frac{A}{\rho} \tag{28}$$

where A is a constant of integration.

From Eq. (28), we have $\rho(v - S) = A$ which gives

$$\rho_1(v_1 - S) = A = \rho_2(v_2 - S) \tag{29}$$

where $\rho_1 = \rho(-\infty)$, $\rho_2 = \rho(+\infty), v_1 = \bar{V}\left(\frac{\rho_1}{1+\delta}\right)$ and $v_2 = \bar{V}\left(\frac{\rho_2}{1+\delta}\right)$.

Hence, speed of travelling wave is given by

$$S = \frac{\rho_1 v_1 - \rho_2 v_2}{\rho_1 - \rho_2} \tag{30}$$

Substituting Eq. (28) into Eq. (27) and rearranging the terms, we get

$$-T(v - S)\big(v - S - c\lambda(1+\delta)\big)\frac{\partial \rho}{\partial x} = q_e(\rho) - \rho S - A \tag{31}$$

Let $q_e(\rho) - \rho S - A = g(\rho)$ (say)
At $\rho = \rho_1$ and $\rho = \rho_2$, $\frac{\partial \rho}{\partial x} = 0$ which gives

$$g(\rho_1) = g(\rho_2) = 0 \tag{32}$$

For a concave function $q_e(\rho)$, $q_e''(\rho) < 0$. This means $g''(\rho) < 0$ and hence, $g(\rho)$ is also a concave function. From Eq. (32) it is easy to prove that $g(\rho) > 0, \forall \rho \in (\rho_1, \rho_2)$. This leads to the conclusion that for existence of traveling wave solution the following condition should be satisfied.

$$-T(v-S)(v-S-(1+\delta)\lambda c)\frac{\partial \rho}{\partial x} > 0 \tag{33}$$

For $\frac{\partial \rho}{\partial x} > 0$ within (ρ_1, ρ_2), the following inequality should hold.

$$-T(v-S)(v-S-(1+\delta)\lambda c) > 0 \tag{34}$$

which gives the condition for existence of traveling wave solution as

$$v-(1+\delta)\lambda c < S < v \tag{35}$$

The condition (35) reduces to the one obtained by Jiang *et al.*[8] when $\delta = 0$ and $\lambda = 1$. If condition (35) is violated at some value $\rho^* \in (\rho_1, \rho_2)$, then $\frac{\partial \rho}{\partial x}$ becomes infinite at ρ^* and we do not get a single-valued solution, which is physically meaningless and it should be replaced by a weak discontinuous solution called shock.

4. Numerical Scheme

Due to the hyperbolic nature of the system of partial differential equations of the proposed model, a more accurate numerical scheme is one that takes into account certain phenomena like propagation of information along characteristic curves, formation of shock and rarefaction waves which are inherent in the nature of hyperbolic systems. Here, we use a conservative finite difference scheme for finding numerical solutions. The importance of using a conservative scheme lies in the fact that these schemes preserve the physical properties of the hyperbolic systems like conservation of physical quantities to a good extent as compared to non-conservative schemes.

The roadway is divided into M sections of length Δx and time domain is divided into J time steps with Δt as the length of each time interval. Applying conservative finite-difference scheme[23] to the system of equations (9), we get the following difference equation

$$U_i^{n+1} = U_i^n - \frac{\Delta t}{\Delta x}\left[\hat{f}_{i+1/2}^n - \hat{f}_{i-1/2}^n\right] + S(U_i^n)\Delta t \tag{36}$$

where indices i and n denote the road segment and time interval, respectively. In Eq. (36), the quantity $\hat{f}_{i+1/2}^n = \hat{f}(U_i^n, U_{i+1}^n)$, which is the local Lax-Friedrichs flux, is given by

$$\hat{f}_{i+1/2}^n = \frac{1}{2}\left[f(U_i^n) + f(U_{i+1}^n) - \alpha^{(n)}(U_{i+1}^n - U_i^n)\right] \tag{37}$$

Here, $\alpha^{(n)} = \max\{|f'(U^n)|\}$ is computed at the beginning of each time step.

The necessary condition of stability and convergence for any explicit finite difference scheme is the Courant, Friedrichs and Lewy (CFL) condition, which requires

$$\left|\alpha^{(n)}\frac{\Delta t}{\Delta x}\right| \leq 1 \tag{38}$$

Hence, Δt is chosen such that it satisfies $\Delta t \leq \frac{\Delta x}{\alpha^{(n)}}$.

In the traffic flow, usually two kinds of boundary conditions closed (periodic) and open (free) are used. Free boundary conditions are sub-divided into transmissive and reflective boundary conditions. Transmissive boundary conditions are employed where the information is being propagated through the end points of the domain while reflective boundary conditions are employed where the information is reflected back into the domain from the boundary points. We proceed with the numerical simulations by employing transmissive boundary conditions at the free boundary points.

4.1. *Shock and rarefaction waves*

To investigate congestion and dissipation of the traffic flow, we carried out numerical test using the aforementioned scheme. Let us consider a road of length L km, initially having two Riemann conditions, one describing congested upstream with nearly free flow downstream and vice versa. The initial conditions are

$$\rho(x,0) = \begin{cases} 0.04; & 0 < x < \frac{L}{4} \\ 0.18; & \frac{L}{4} \leq x < \frac{3L}{4} \\ 0.04; & \frac{3L}{4} \leq x < L \end{cases} \tag{39}$$

Eq. (36) corresponds to the two realistic situations in traffic flow: appearance of shock waves when free-flow traffic meets nearly stopped vehicles and the other is just opposite and describes the rarefaction wave as a queue dissolves. The distance $L/4$ is relatively large for representing the waves distinctly. For initial conditions of velocity, we assume

$$v(x,0) = \bar{V}\big(\rho(x,0)\big) \tag{40}$$

where $\bar{V}(\rho) = v_f\left[1 - exp\left(1 - exp\left(\frac{c_m}{v_f}\left(\frac{\rho_m}{\rho} - 1\right)\right)\right)\right]$ is the modified equilibrium speed-density relationship[24]. Here, v_f and c_m are the free flow speed and the kinematic wave speed under jam density ρ_m, respectively. Free boundary conditions are adopted and the calculations are performed using the following set of parameters[18]:

$$v_f = 30 \text{ m/s}, \rho_m = 0.2 \text{ veh/m}, T = 10 \text{ s}, c_m = 11 \text{ m/s}, \\ \lambda = 1, L = 40 \text{ Km}, \Delta x = 200 \text{ m and } \Delta t = 1 \text{ s} \tag{41}$$

Figs. 2(a) and 2(b) shows how traffic waves evolve under the effect of Riemann conditions (36). It is easy to check that when a low density traffic stream meets high density stream at $L/4$, the condition (35) is not satisfied for all possible values of δ. As a consequence, a backward moving shock wave appears and its propagation speed is found to be negative. Similarly, we can observe the evolution of a rarefaction wave front at $3L/4$ which is smoothed over time as the condition (35) is satisfied and is consistent with the real traffic situation. The LSD parameter δ does not play a crucial role in the evolution of shock and rarefaction waves. Further, it can be concluded from Fig. 2 that the proposed model validates the aforementioned theoretical predictions.

4.2. *Effect of lateral separation distance parameter*

On the basis of linear stability analysis, we make a numerical study to verify and visualize the effect of lateral separation distance parameter for the proposed model. Let us consider the behavior of a localized perturbation on an initially homogeneous road of length L=32.2 km.

$$\rho(x,0) = \rho_h + \Delta\rho\left\{cosh^{-2}\left(\frac{160}{L}\left(x - \frac{5L}{16}\right)\right) - \frac{1}{4}cosh^{-2}\left(\frac{40}{L}\left(x - \frac{11L}{32}\right)\right)\right\} \quad x \in [0, L] \\ v(x,0) = \bar{V}\big(\rho(x,0)\big) \quad ; x \in [0, L] \tag{42}$$

Here, ρ_h and $\Delta\rho$ are the homogeneous density and the amplitude of perturbation, respectively. To describe the amplification of small disturbances, periodic boundary conditions are adopted and the relationship proposed by Kerner and Konhäuser[5] is used as the equilibrium speed-density function.

$$\bar{V}(\rho) = v_f \left[\left(1 + exp\left(\frac{\frac{\rho}{\rho_m} - 0.25}{0.06} \right) \right)^{-1} - 3.72 \times 10^{-6} \right] \quad (43)$$

4.2.1. *Fundamental diagram*

The flow-density relations in Fig. 3 give insight about the characteristics of the non-lane-based homogeneous continuum model. It is clear from Fig. (3) that δ almost has no effect on flow at low densities but does have significant effects inside the critical region, where the flow increases with an increase in δ. Analogously to the free flow, δ has very little effect on the flow near the jam density. This can be understood as follows. In low density traffic conditions, the drivers have sufficient free space to drive nearly at their desired speeds and the lateral separation distance between the vehicles is almost irrelevant for the drivers in this case. This is in contrast to the intermediate density region, where the lateral separation distance plays a significant role in the driving behavior as the interactions between the vehicles are strong and hence increases the flow. At density near to jam density, lateral space shrinks as vehicles are close to each other and the magnitude of δ is sufficiently small to affect the flow.

4.2.2. *Region of instability*

The effect of lateral separation distance on the instability region, which can be computed using Eq. (24), is shown in Fig. 4. An important consequence is that the instability region shrinks with increase in , which means that higher value of lateral separation can stabilize the traffic conditions and maximize the flow. As an example, when $\rho_h = 0.05\ veh/m$, traffic is in free flow state for $\delta = 0.5$ in contrast to congested state for $\delta = 0$. These results are in accordance with the stability results obtained for a two-lane car-following model[25]. Note that the critical region shifts towards right with increase in δ. It can be justified as the equilibrium curves shifted towards right with the increase in δ.

4.2.3. *Local cluster effect*

To analyze the effect of δ on the non linear local cluster effect in traffic flow, we investigate the traffic density pattern with respect to time. Figs. 5 and 6 describe the spatio-temporal evolution of density waves in the critical region for two different values of ρ_h, respectively. It is evident that inside the critical region, the initially homogeneous state of traffic flow is unstable with respect to the growth of any non-homogeneous perturbations with small enough amplitude. Fig. 5 shows various density patterns for different values of δ when the initial density is just above the down critical density. As the instability condition (35) is satisfied, the patterns (a), (b), (c) and (d) are unstable and small disturbances propagate quickly leading to traffic congestion. It is also clear from Fig. 5 that the cluster in situation (a) is more complex than in (b), and in (c), more complex than in (d) because the amplitude of density wave decreases with increase in lateral separation. This situation corresponds to stop-and-go traffic. Finally, due to the continuous shifting and shrinking of the unstable region, the initial homogeneous density becomes less than the down critical density at $\delta = 0.4$ and as a result the effect of the perturbation dies out with respect to time and traffic flow becomes stable (Fig. 5(e)). This result matches with theoretical result obtained using linear stability analysis (Eq. 24). One can see from Fig. 4 that the homogeneous density $\rho_h = 0.048\ veh/m$ lies inside the region of instability for $= 0, 0.1, 0.2, 0.3$, while for $\delta = 0.4$, it lies inside the stable region.

A reverse effect is obtained when the initial density is chosen just greater than the up critical density (Fig. 6). Fig. 6(a) depicts that initial disturbance will die out with time when the density is just above the up critical density. As δ parameter increases, the initial small perturbation grows in time. This

is due to the shift in unstable region towards right. It is clear from the Fig. 6 that further increase in the value of δ will lead to more complex clusters.

From the above results, it is found that the simulation results are in good agreement with the analytical ones. Both numerical and analytical results have shown that the lateral separation has a considerable effect on the properties of traffic flow i.e. stability, the jamming transition and fundamental diagram. The results also give an insight to eliminate traffic bottlenecks and increase the flow by widening lanes even in lane-based system.

5. Heterogeneous Model

To check whether the proposed non-lane-based continuum model will be able to correctly replicate the heterogeneous traffic flow characteristics, we conduct numerical study on the fundamental diagram with various proportions of two types of vehicles i.e. cars and buses. The characteristics of heterogeneous traffic jam density and total flow can be generalized with the similar idea of homogeneous traffic flow. The jam density on a homogeneous traffic flow for non-lane-based system can be defined as follows:

$$\rho_m = \frac{1+\delta}{l+h} \tag{44}$$

where l and h are respectively the length and safety distance of the vehicle. The generalization of the safety distance h_i for i-class in a heterogeneous case is complex as it is related to the probability and the characteristics of the front vehicle. Since p_j is the probability that the vehicle in front of the i-class is j-class, so h_i can be computed as a mean of the random variables h_{ij} as

$$h_i = \sum_{j=1}^{N} p_j h_{ij} \tag{45}$$

Here, h_{ij} is the i-class safety distance when its front vehicle is j-class and satisfies $h_{im} > h_{in}$if $v_{im} > v_{in}$. Since, vehicles are distributed randomly on the roadway, the vehicle length and safety distance of the whole system will be a random variable and can be calculated as $l = \sum_{j=1}^{N} p_j l_j$, $h = \sum_{j=1}^{N} p_j h_j$ where l_j is the length of the j-class vehicle. Now, Eq. (44) can be generalized to compute the jam density in the heterogeneous case as

$$\rho_m = \frac{1+\delta}{\sum_{j=1}^{N} p_j (l_j + h_j)} \tag{46}$$

Since the computation of the proportion $p_j(x,t)$explicitly is complex and related to the j-class density at the point (x,t), total density and the structure of the heterogeneous traffic, we adopted the approach proposed by Tang *et al.*[20]. For the numerical experiment, we consider two classical equilibrium functions for each i-class. One is the maximization sensitivity curve given by Del Castillo *et al.* [24],

$$\bar{V}_i(\rho) = v_{if}\left[1 - exp\left(1 - exp\left(\frac{c_{im}}{v_{if}}\left(\frac{\rho_m}{\rho} - 1\right)\right)\right)\right], \tag{47}$$

and the other is the Kerner and Konhäuser equilibrium function[5],

$$\bar{V}_i(\rho) = v_{if}\left[\left(1 + exp\left(\frac{\frac{\rho}{\rho_m} - 0.25}{0.06}\right)\right)^{-1} - 3.72 \times 10^{-6}\right] \tag{48}$$

Here, ρ is the total density.

In this experiment, we consider a highway of length 20 km with open boundary conditions. For simplicity, we assume that the heterogeneous traffic consists of only two classes ($i = 1$ and 2 represents car and bus, respectively) and the parameters relevant to these classes are set as follows[18]:

$h_{11} = h_{12} = 2$ m, $h_{21} = h_{22} = 1$m, $c_{1m} = c_1 = 11$s, $c_{2m} = c_2 = 7$s, $T_1 = 10$s, $T_2 = 15$s, $v_{1f} = 30$ m/s, $v_{2f} = 20$ m/s, $l_1 = 3$ m, $l_2 = 10$ m, $\tau_1 = 7$ m/s, $\tau_2 = 10$ m/s (49)

Fig. 7 represents the change in the total density with respect to the car proportion for different values of δ. The jam density increases with the increase of the proportion of car. It is also clear from the figure that δ parameter also enhances the jam density, which means that utilization of lateral space reduces the traffic congestion.

5.1. *Maximization sensitivity equilibrium function*

We study the effect of proportions of car and bus and lateral separation on fundamental diagram of the heterogeneous traffic. The results are plotted in the Fig. 8 and following conclusions are made.
(a) The jam density decreases with the decrease of car proportion.
(b) For very small total density, the proportion of car has almost no effect on the mean total flow as the traffic is in free flow phase and both classes of vehicles can move freely without interacting each other.
(c) The total flow as well as the instability region decreases sharply with the increase of bus proportion. These results are in good accordance with the results of Tang *et al.*[20].
(d) The δ parameter plays an important role to enhance the total flow for any vehicle proportions.

5.2. *The Kerner and Konhäuser equilibrium function*

For various different proportions of car & bus, the fundamental diagram of the heterogeneous traffic is plotted in Figs. 9(a) and 9(b) with respect to $\delta = 0$ and $\delta = 0.2$ and the following results are obtained.
(a) For small density, the results are similar to the Del Castillo model i.e. the proportion of car has almost no effect on the mean total flow.
(b) The total flow as well as the instability region decreases sharply with the increase of bus proportion.
(c) The δ parameter enhances the total flow for any vehicle proportions.
(d) For high density, the effect of vehicle proportion as well as the effect of lateral separation becomes irrelevant as the total flow approaches to zero near jam density asymptotically. This result is not consistent with the result of maximum sensitivity curve.

6. Conclusion

In this paper, a generic continuum model for heterogeneous traffic flow without lane discipline undertaking lateral separation into account is developed. Non-lane-based full velocity difference car following model given by Jin *et al.*[16] is first extended to heterogeneous case and then the relationship between micro and macro variables is applied to obtain a non-lane-based generic continuum model for heterogeneous traffic flow. To discuss the effect of lateral separation, the qualitative properties for the homogeneous case are examined analytically as well as numerically. It is shown that the effects of the lateral separation stabilized the traffic flow by shrinking the instability region. For heterogeneous traffic flow, two different types of equilibrium functions are considered and the effect of lateral separation parameter on various proportions of heterogeneous traffic consists of car and bus is discussed. Our theoretical and numerical findings are in good agreement which shows that our model can describe some qualitative properties of the heterogeneous traffic for non-lane-based system accurately.

Apart from this, the present work needs to be explored further comprehensively. The proposed model has the following limitations.

1. The driver's heterogeneity is not considered or incorporated in this paper. We have classified traffic only in terms of type of vehicle.
2. The qualitative properties of the model for heterogeneous case have not been discussed.

Acknowledgements

The second author acknowledges Council of Scientific and Industrial Research (CSIR), New Delhi, India for providing financial support.

References:

1. M. J. Lighthill and G. B. Whitham, *Proc. R. Soc. Lond. Ser. A* **229**, 317 (1955).
2. P. I. Richards, Oper. Res. **4**, 42 (1956).
3. H. J. Payne, *Mathematical Models of Public Sys.1 - Simulation Council Proceedings* 51 (1971).
4. C. F. Daganzo, *Trans. Res. B* **29**, 277 (1995).
5. B. S. Kerner and P. Konhäuser, *Phys. Rev. E* **48**, 2335 (1993).
6. H. M. Zhang, *Trans. Res. B* **32**, 485 (1998).
7. A. Aw and M. Rascle, *SIAM J. Appl. Math.* **60**, 916 (2000).
8. A. K. Gupta, *Int. J. Mod. Phys. C* **24**, 1350018 (2013).
9. R. Jiang, Q. S. Wu and Z. J. Zhu, *Trans. Res. B* **36**, 405 (2002).
10. S. P. Hoogendoorn and H. L. Bovy, *Trans. Res. Rec.* **1678**, 150 (1999).
11. G .C. K. Wong and S. C. Wong, *Trans. Res. A* **36**, 827 (2002).
12. D. Ngoduy, S. P. Hoogendoorn and J.W.C. Van Lint, *Trans. Res. Rec.* **1923**, 73 (2005).
13. J. A. Laval and C. F. Daganzo, *Transp. Res. B* **40**, 251 (2006).
14. A. K. Gupta and V. K. Katiyar, *Transportmetrica* **3**, 73 (2007).
15. S. Logghe and L. H. Immers, *Transp. Res. B* **42**, 523 (2008).
16. S. Jin, D. Wang, P. Tao and P. Li, *Physica A* **389**, 4654 (2010).
17. R. Nair, H. S. Mahmassani and M. H. Elise, *Transp. Res. B* **45**, 1331 (2011).
18. G. H. Peng, X. H. Cai, B. F. Cao and C. Q. Liu, *Phys. Lett. A* **375**, 2823 (2011).
19. B. Gunay, *Transp. Res. B* **41**, 722 (2007).
20. T. Q. Tang, H. J. Huang, S. G. Zhao and H. Y. Shang, *Phys. Lett. A* **373**, 2461 (2009).
21. R. J. LeVeque, Finite Volume Methods for Hyperbolic Problems, ed. 31 (Cambridge University Press, 2002).
22. Z. H. Ou, *Physica A* **351**, 620 (2005).
23. P. Zhang, R. X. Liu and S. C. Wong, *Phys. Rev. E* **71**, 056704 (2005).
24. J. M. Del Castillo and F. G. Benitez, *Transp. Res. B* **29**, 373 (1995).
25. T. Q. Tang, H. J. Huang and Z. Y. Gao, *Phys. Rev. E* **72**, 066124 (2005).

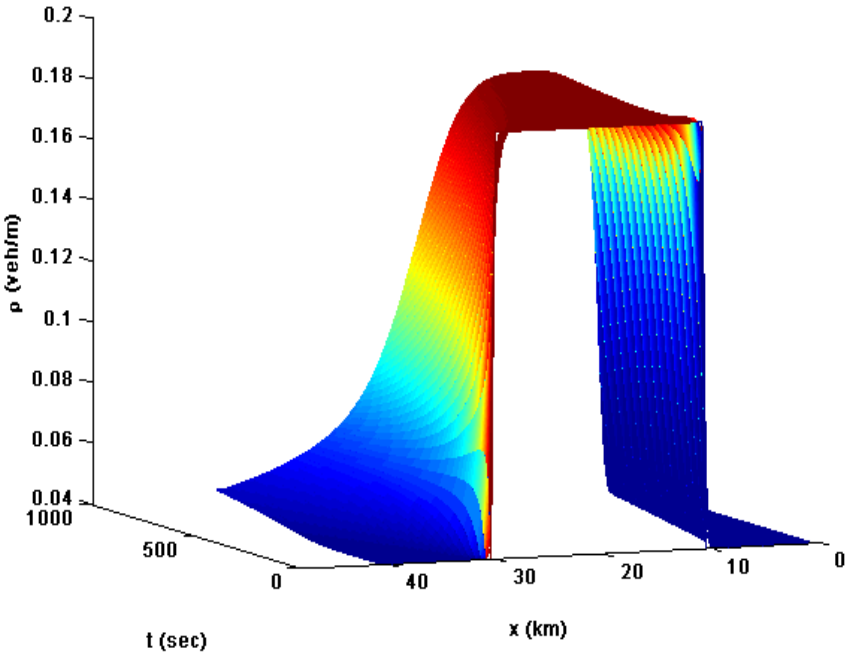

2(a)

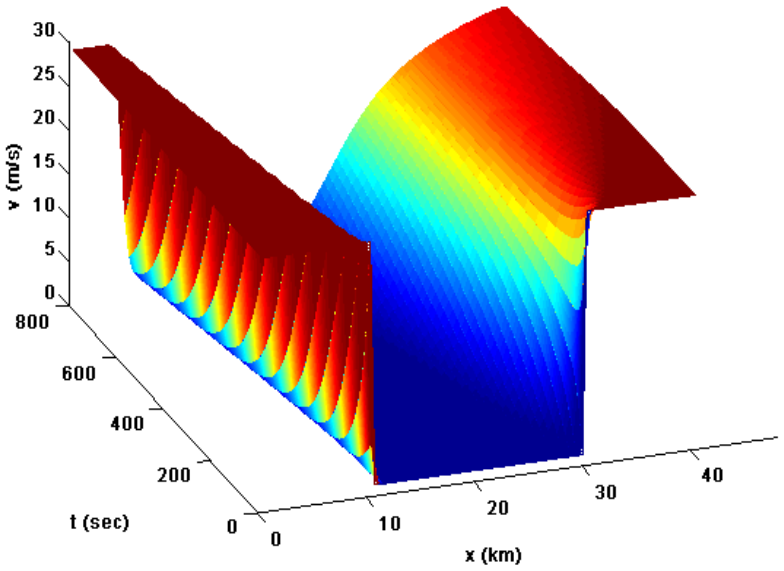

2(b)

Fig. 2. Shock and rarefaction waves under Riemann initial condition (36): (a) temporal development of density $\rho(x,t)$ (b) temporal development of speed $v(x,t)$.

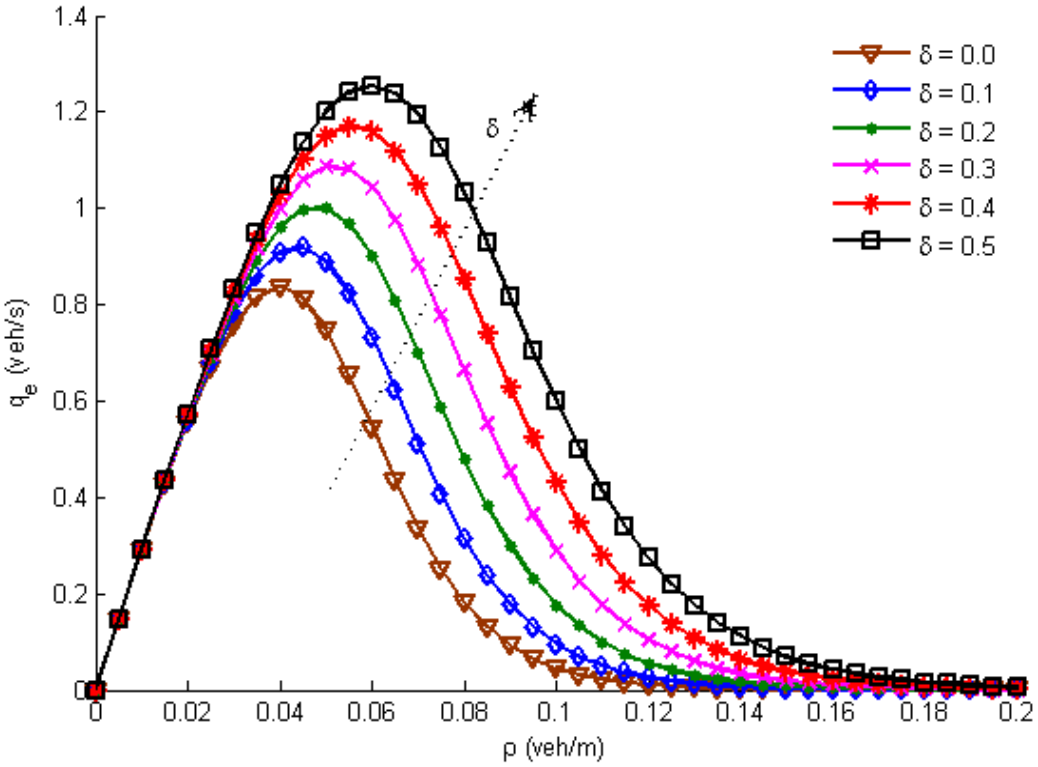

Fig. 3. Fundamental diagram for different values of lateral separation distance parameter.

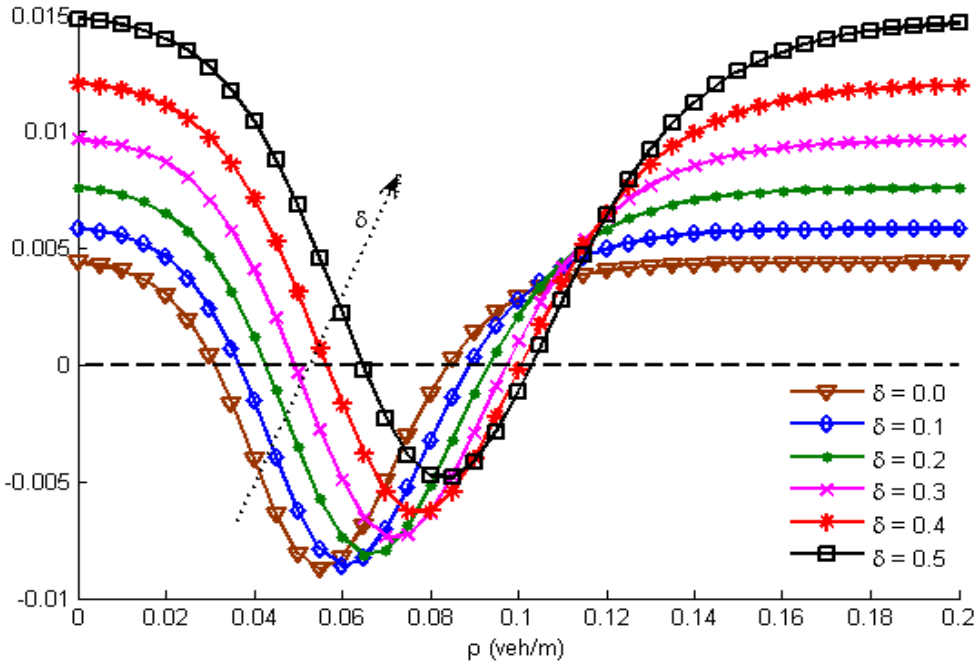

Fig. 4. Stability region for different values of lateral separation distance parameter.

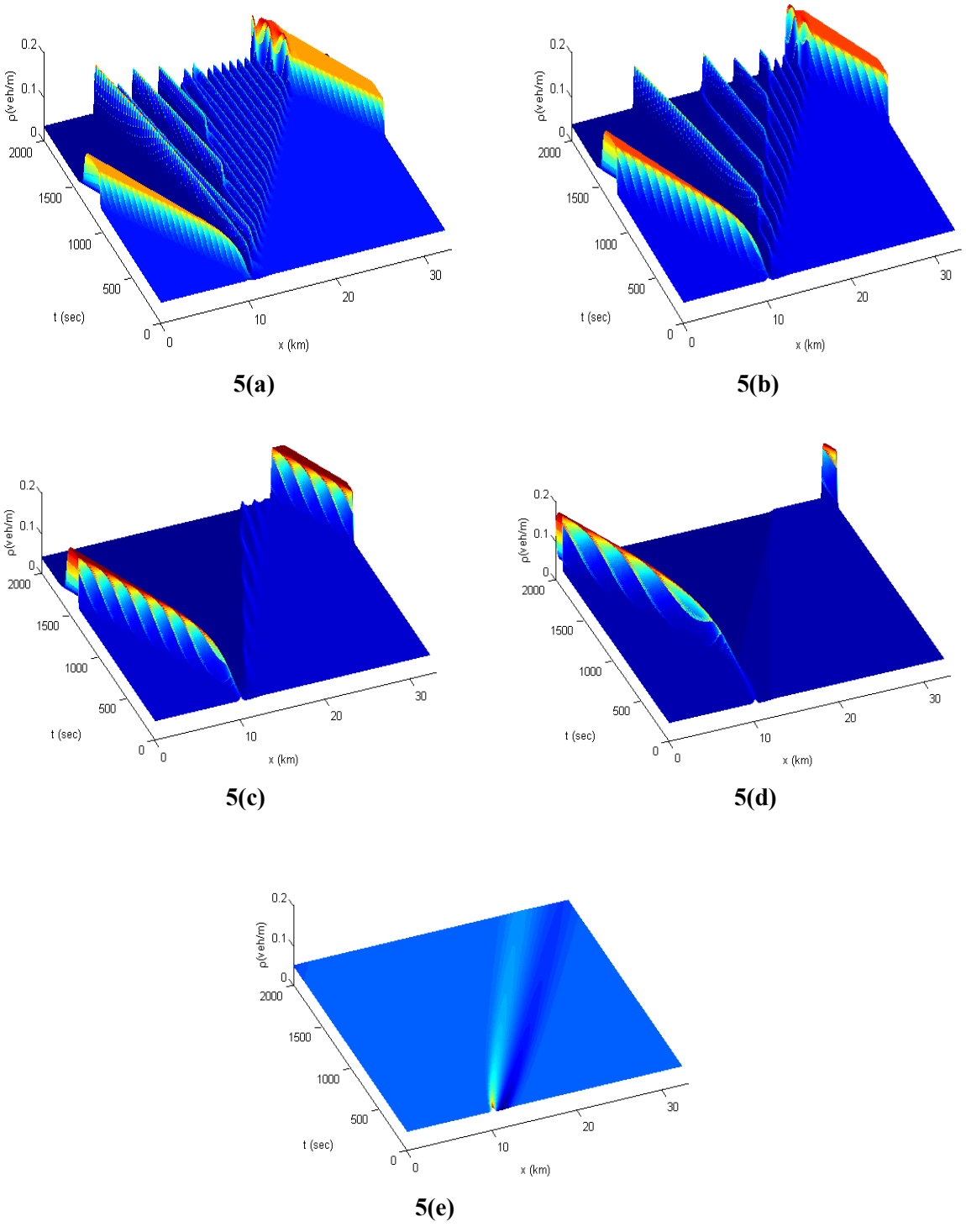

Fig. 5. Temporal evolution of traffic density with a homogeneous traffic density $\rho_h = 0.048$ veh/m and a localized perturbation of amplitude $\Delta\rho = 0.01$ veh/m (a) $\delta = 0$; (b) $\delta = 0.1$; (c) $\delta = 0.2$; (d) $\delta = 0.3$; (e) $\delta = 0.4$

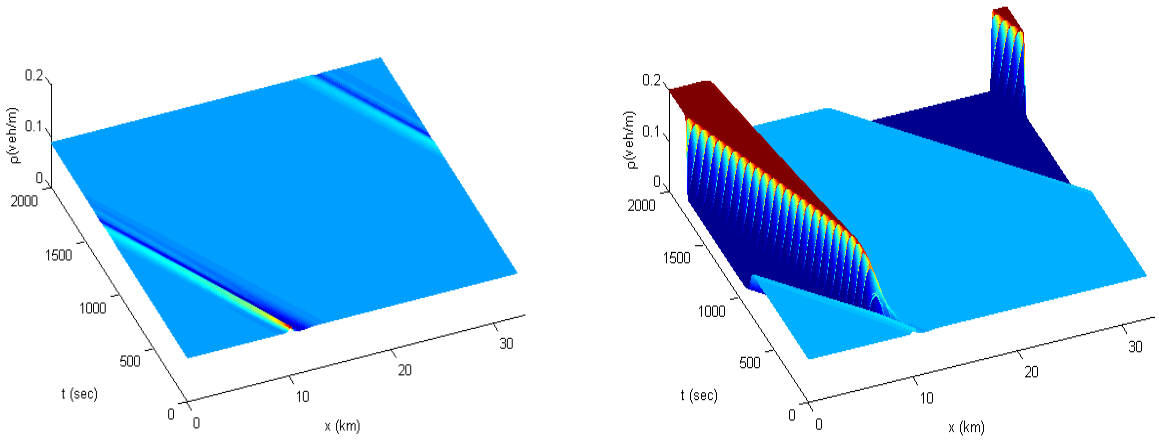

6(a) **6(b)**

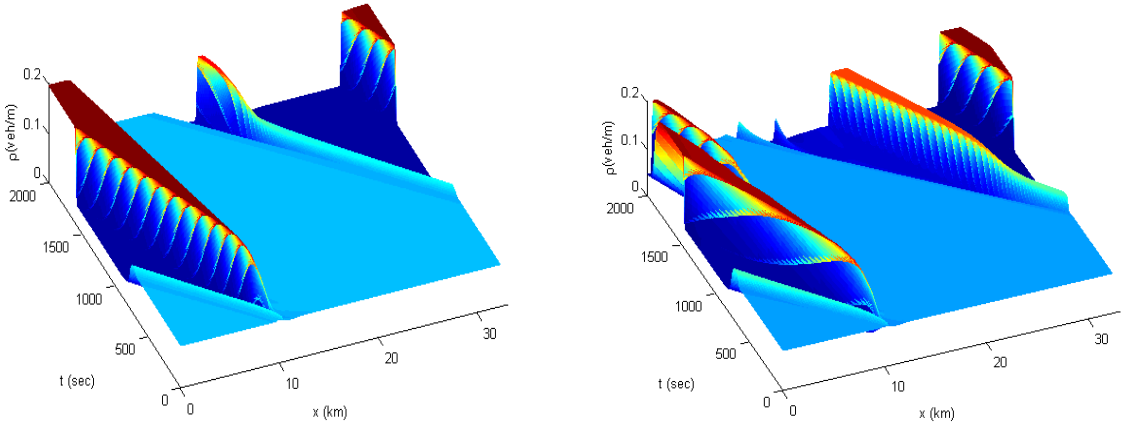

6(c) **6(d)**

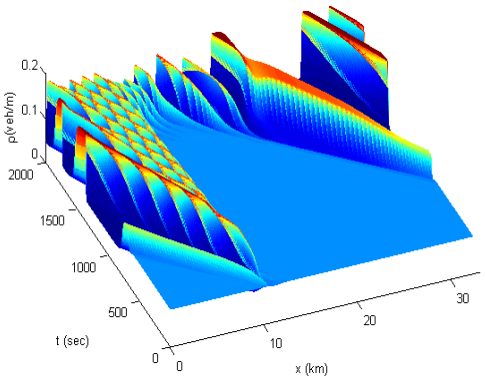

6(e)

Fig. 6. Temporal evolution of traffic density with a homogeneous traffic density $\rho_h = 0.085$ veh/m and a localized perturbation of amplitude $\Delta\rho = 0.01$ veh/m (a) $\delta = 0$; (b) $\delta = 0.1$; (c) $\delta = 0.2$; (d) $\delta = 0.3$; (e) $\delta = 0.4$

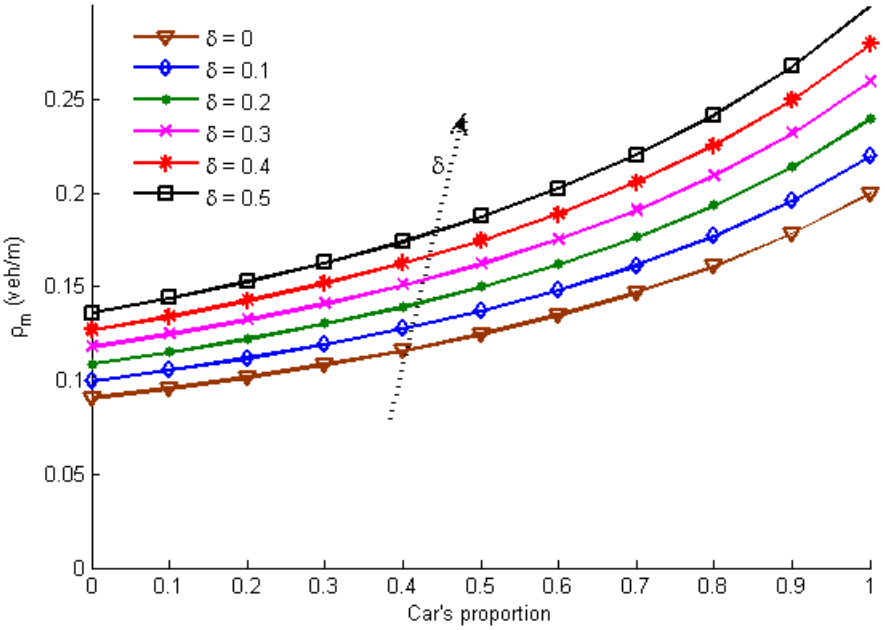

Fig. 7. Jam density for different values of lateral separation distance parameter.

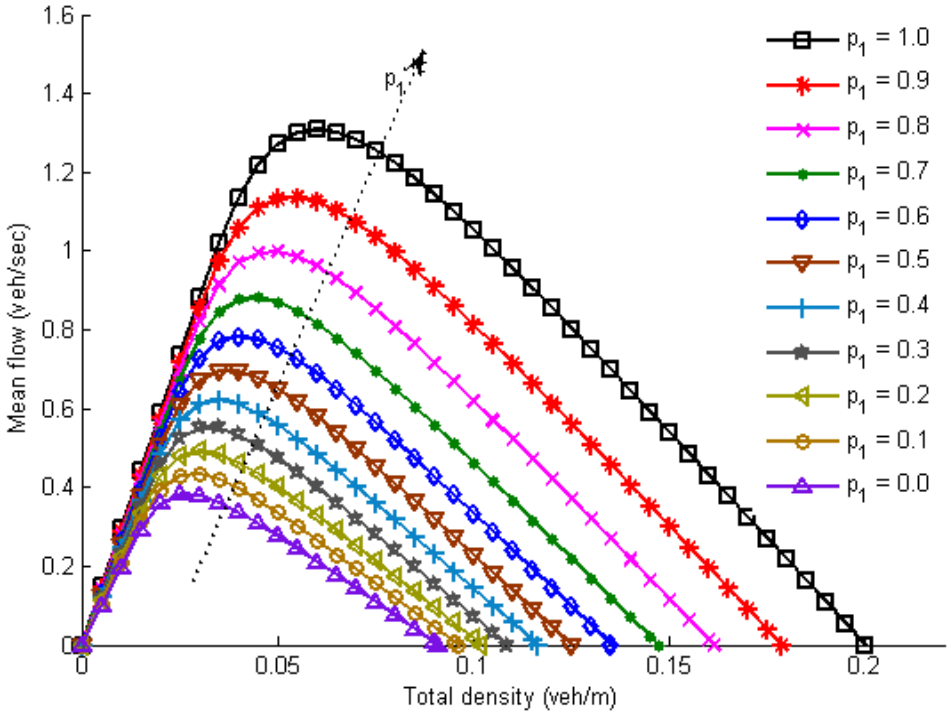

8(a)

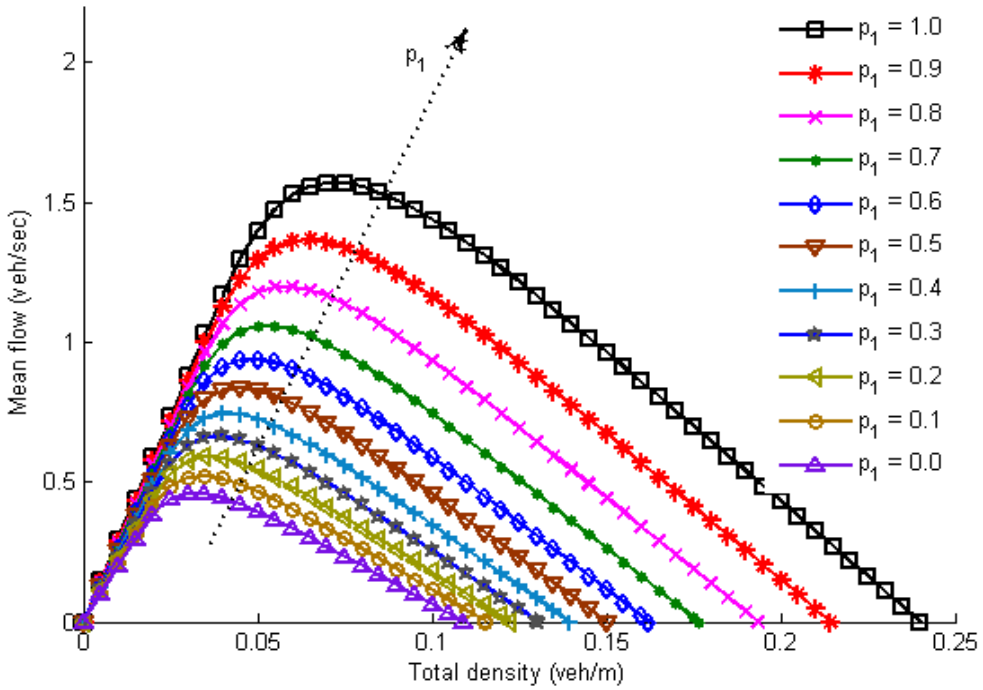

8(b)

Fig. 8. The fundamental diagram of heterogeneous traffic flow using Del Castillo model for different proportions of car: (a) $\delta = 0$; (b) $\delta = 0.2$. Here, p_1 represents the proportion of car.

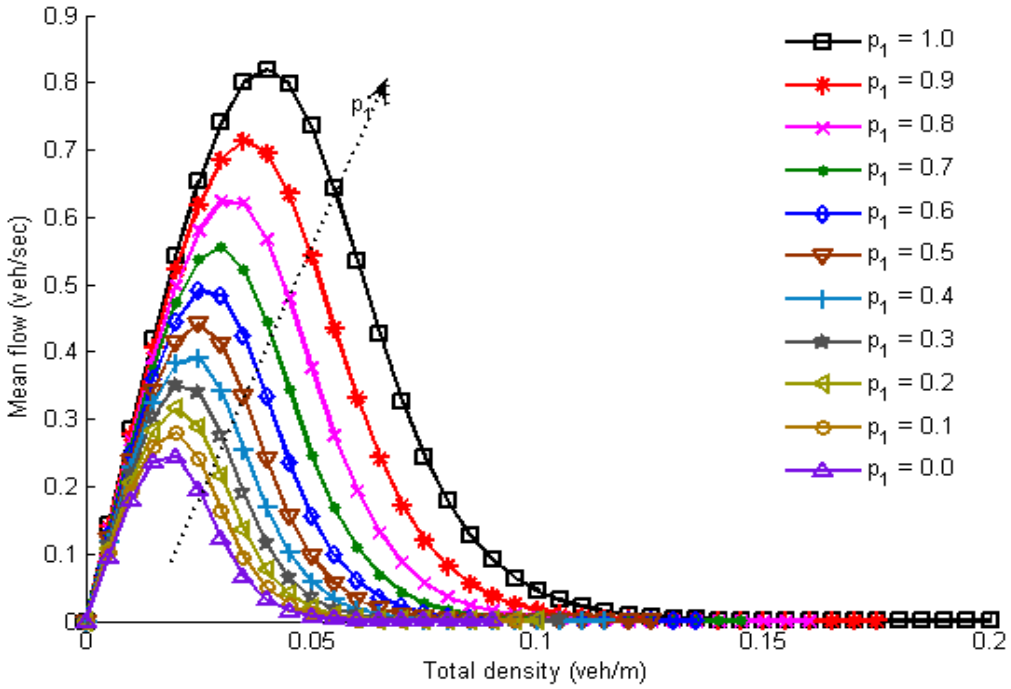

9(a)

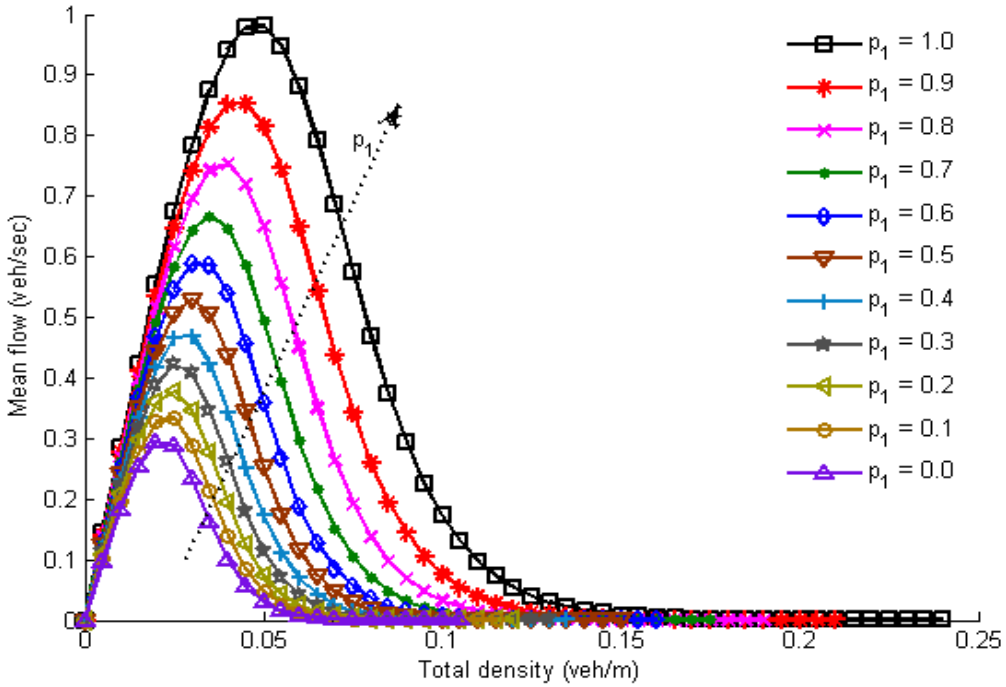

9(b)

Fig. 9. The fundamental diagram of heterogeneous traffic flow using Kerner and Konhäuser model for different proportions of car: (a) $\delta = 0$; (b) $\delta = 0.2$. Here, p_1 represents the proportion of car.